Improving 6G Network Spectrum Efficiency with Non-Cooperative and Cooperative Spectrum Sharing Using NOMA and Massive-MIMO

Mohamed Hassan[1*], Manwinder Singh[2], Khalid Hamid[3], Imadeldin Elsayed[4]

[1]Department of Wireless Communication, Lovely Professional University, Punjab 144001, India
[2]Department of Wireless Communication, Lovely Professional University, Punjab 144001, India
[3] Department Electronics and Communication, University of Science & Technology, Sudan
[4]Department Electrical and Electronic Engineering, University Malaysia Pahang, Pahang, Malaysia

Abstract

There is an expectation that standards for sixth-generation (6G) wireless communication networks in the future will give previously unheard-of speeds for the flow of information as well as spectrum optimization. This will present new issues for 6G networks. Non-orthogonal multiple access (NOMA) is one of the most efficient ways to boost the spectrum efficiency (SE) of a 6G network. The most promising contemporary technologies, such as cognitive radio (CR) and multiple access, can be used to improve SE. When NOMA's network-oriented multi-access capabilities are combined with those of the Cognitive Radio Network (CRN), a new era of efficient communication is expected to dawn. To improve the spectral efficiency (SE) of the NOMA DL power domain (PD), this work presents two distinctive strategies that are used in conjunction with un-cooperative and cooperative CRN (Un-CCRN and CCRN) if one primary user (PU) is unable to receive through the dedicated channel due to interference or noise. Users' distances, power placement coefficients, and transmit powers (TPs) vary across the proposed three network topologies, and over the proposed three network sizes of 128x128, 256x256, and 512x512 Massive Multiple Input Multiple Output (M-MIMO). Performance is analyzed while simultaneously considering channel instability and successive interference cancellation (SIC). The channels of fading are modelled after frequency-dependent Rayleigh fading. MATLAB is used to determine the proposed model's SE. With 128x128, 256x256, and 512x512 M-MIMO integrated into the DL NOMA system, the system's SE performance is improved by 73%, 82%, and 87%, respectively; with the Un-CCRN NOMA model, the improvement is 75%, 83%, and 88%; and with the CCRN-NOMA model, the improvement is 75.8%, 84%, and 88.3%. The SE is significantly improved by employing M-MIMO technology. The acquired expressions agree with the outcomes of the provided Monte Carlo simulations, providing further evidence for the validity of our investigation.

*Corresponding author. Email: mhbe4321@gmail.com

1. Introduction

The sixth generation (6G) represents the next phase of wireless technology, which includes network densification, enhanced throughput, increased reliability, lower power consumption, ubiquitous connectivity, and the introduction of new services such as artificial intelligence, smart wearables, implants, autonomous vehicle driving and computational reality devices. and 3D sensing and mapping [1]. According to academic discourse, a critical prerequisite for the development of 6G wireless networks is the ability to effectively manage large amounts of data and facilitate communication at an exceptionally high data rate for each individual device [2].

In order to achieve the goals of the sixth generation and address the obstacles of the fifth generation in accommodating emerging requirements, it is necessary to improve the use of spectrum and develop strategies to mitigate the difficulty of spectrum scarcity, which constitutes an obstacle to sustainable progress in this field.

Non-orthogonal multiple access, also known as NOMA, enables a large number of users to share the same time and frequency resources by utilizing something else, such as power or code, which causes signals from different users to travel in different directions and cause interference with each other. This makes it possible for multiple users to share the same time and frequency of resources. This is accomplished by utilizing anything that, when used by multiple people, causes their signals to interfere with one another and render them unusable. The power domain (PD) NOMA, also known as PD NOMA, and the code domain NOMA, also known as CD NOMA, are two more, more general types of NOMA that have been found [3-4-5-6-7-8].

Multiplexing user signals within the PD helps NOMA accomplish its objective of achieving the highest possible level of spectral efficiency (SE) in 6G networks.

This is made possible by employing superposition coding (SC) at the transmitter and sequential interference cancellation (SIC) at the receiver, respectively. Because power domain NOMA can still achieve a large performance improvement [9–10–11–12], the latency of channel status information (CSI) feedback shouldn't be a problem, and neither should the mobility of the user equipment (UE). The ability of a transmitter to efficiently allocate broadcast power and pair users depends on the transmitter having information about the CSI of each receiver.

The concept of "cognitive radio" (CR) pertains to a technique employed to enhance the efficacy of spectrum utilisation. This approach aims to designate a certain method of wireless communication. The acronym "CR" denotes a wireless communication technique wherein a transceiver uses data to identify the occupied and unoccupied communication channels, afterwards transitioning to the unoccupied channels while evading the occupied ones [13-14-15]. The abbreviation "CR" is derived from the term "channel hopping".

CR is distinct due to two primary characteristics. Intellectual capacity is the ability of an organism to comprehend information in its radio environment; re-configurability is what permits spectrum awareness. In the first place, there is spectrum awareness, which is enabled by intellectual capacity. Because of its "re-configurability," CRs are able to instantly adjust their operational capabilities in response to shifting radio conditions. Spectrum sensing, spectrum management, spectrum sharing, and spectrum traffic are the fundamental functionalities of CR; however, each of these core features has a number of accompanying methods [13-16-17]. Spectrum traffic is a term that refers to the flow of information across the spectrum.

If the radio spectrum is shared, cognitive and simple radio licenses can coexist without interference. Because of this, the frequency will become significantly more useful. There are a couple of ways that one can go about

accomplishing this objective, including through cooperation and non-cooperation.

The new strategy developed by NOMA is just now being implemented by CR Systems. These developing technologies, when coupled, have the ability to simplify the design of power allocation, drastically boost spectrum efficiency (SE), and continuously meet the needs of consumers for higher-quality service [18–19].

The fundamental studies [20–21] have demonstrated that the positive effects of multipath propagation can be effectively mitigated by using a considerable number of antennas and sending out multiple signals from both the transmitter and receiver. In a wireless network, enabling massive multiple-input, multiple-output (M-MIMO) communication has the potential to improve the SE in 6G system. This goal can be accomplished by increasing the number of antennas used within the network.

Although there is a substantial body of written material on NOMA and CR, only a small number of studies have properly demonstrated the capabilities of CR-based NOMA systems. However, there is widespread agreement among industry professionals that the integration of such technologies will play an important role in solving the large network requirements that 6G and subsequent generations will impose. As a result, it is our responsibility to provide a comprehensive answer to the question of how to combine CR-based NOMA technology with M-MIMO to ensure improved network performance. A significant contribution has been generated as a result of the work described in this study, and will be summarized as follows:

a. Spectral Efficiency Improvement: The suggested concept aims to greatly improve spectral efficiency in 6G communication networks. Combining technologies like NOMA, M-MIMO, and CRN results in a significant increase in the capacity to transmit data more efficiently within the same bandwidth.

b. Integration of Emerging Technologies: The report recommends incorporating emerging technologies such as NOMA and M-MIMO into 6G networks. This is a novel technique to dealing with the issues of future wireless networks.

c. Detailed Quantitative Evaluation: The concept is backed up by a detailed quantitative evaluation that takes into account various network topologies and sizes. This gives solid evidence for how these technologies can improve spectral efficiency in real-world settings.

d. Performance elements Considered: The study takes into account crucial elements such as Successive Interference Cancellation (SIC), unstable channels, and the effect of Rayleigh fading on performance. This exhibits a thorough comprehension of real-world problems.

e. The uniqueness of the study is in the quantitative analysis of the performance of the 6G networks under various conditions, as well as the combination of technologies and techniques to increase spectral efficiency.

The author proposes Sunfa Ata Zuyan (SAZ), which extends identification algorithms to slow the lunar phase and

get around earlier difficulties in locating and figuring out the moon's phase. recommending a quicker SAZ method to calculate lunar phase data and assess the Raspberry Pi. contrasting images. The findings show that SAZ aids in the form detection algorithm's discovery of the moon's phases and objects [22].

The author took into account recent advancements in embedded systems when creating the portable Raspberry Pi-based system. The system that was designed takes pictures. After image pre-processing, the moon phase is then declared using the portable Python GUI. Finally, an efficient system was suggested by the special SAZ algorithm [23].

The Handy Pipe Defect (HPD) was developed by the author and the creator of the MIT programmer using the Personal Image Classifier (PIC) as a machine learning technique to process problem names and assist users in investigating and repairing them [24].

This is an important stage in accomplishing our goal. For the rest of the paper, we'll be using this structure: The second section will serve as a retrospective on the preceding and preceding events. In the third section of this study, we examine the mathematical model that has been provided for the system under investigation. The simulation settings are discussed in Section 4. The results of the simulation are examined in Section 5. Future directions for research are discussed in the final section of the study.

2. Related Works

The present study introduces a novel hybrid precoding technique with reduced complexity for downlink multi-antenna, multi-user millimetre-wave (mm-Wave) M-MIMO systems. The purpose of this action was to mitigate any conflicts and disruptions among users. The simulation findings demonstrate that the suggested technique achieves a cumulative SE and BER performance that is close to ideal in both the mm-Wave and Rayleigh channels [25].

The author showed a two-stage plan with centralized resource allocation and distributed power control to meet the requirements of NR V2X Mode 1 with NOMA technology in each vehicle group and a cooperative game approach to control vehicle group power to increase system capacity. The goal of the author's plan was to increase the system's overall capacity. In comparison to the noncompliant game, the communications throughput of the proposed system as well as the amount of TR used are both improved [26]. Energy economic efficiency is a new performance metric that measures the time-average throughput per energy cost. The author has been looking into ways to maximize long-term energy and economic efficiency by optimizing both communication and energy resources. At last, a thorough theoretical analysis is offered, and simulations are used to verify the proposed algorithm in a number of different system configurations [27].

A new serial sub-array activation diversity method is suggested by the author for a large MIMO system that also uses NOMA. The proposed system works better than regular full-array massive MIMO configurations, according to the results of a thorough analytical analysis in which an exact closed-form expression for the chance of an outage was found [28].

The author looked into DL channel estimation for intelligently reflecting surface-assisted massive MIMO systems to lessen the load on the computer and the time it took to train it. This row-sparse, coupling matrix-affected sparse signal recovery problem The advantages of this strategy are demonstrated through numerical simulations [29].

3. System Model

Assume the following scenario: there is a wireless network with six users that use NOMA, denoted as (U1, U2, U3, U4, U5, and U6) as seen in Figure 1. Henceforth, the relative distances between their base stations (BS) will be denoted as follows: Variables d1, d2, d3, d4, d5, and d6 On the basis of the measured distances, it can be concluded that user U1 has the weakest signal strength and is located the farthest from the base station (BS), whereas user U6 has the strongest signal strength and is located the closest to the BS. Let these variables represent the Rayleigh fading coefficients corresponding $|h_1|^2 |h_2|^2 |h_3|^2 |h_4|^2 |h_5|^2 |h_6|^2$. The relevant variables are denoted as x_1, x_2, x_3, x_4, x_5, and x_6. Each entity's power coefficients are denoted as α_1, α_2, α_3, α_4, α_5, and α_6. Based on the concepts of the NOMA PD, it is proposed that those with a greater need for power should possess a relatively smaller amount, while those with a lesser need for power should possess a relatively greater amount. Consequently, modifications must be made to the power coefficients. The sequence of quadrature phase-shift keying (QPSK) messages x_1, x_2, x_3, x_4, x_5, and x_6 intended for transmission to the base stations (BSs) will be examined in this section. Consequently, the provided expression can be expressed as

$$x = \sqrt{p}\left(\sqrt{\alpha_1}x_1 + \sqrt{\alpha_2}x_2 + \sqrt{\alpha_3}x_3 + \sqrt{\alpha_4}x_4 + \sqrt{\alpha_5}x_5 + \sqrt{\alpha_6}x_6\right).$$

The base station (BS) is transmitted the encoded overlay signal.
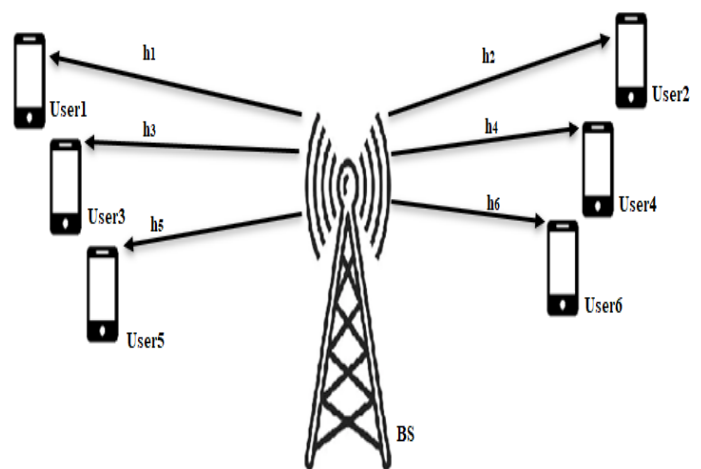

Figure 1. DL NOMA PD network with six users

The signal that exhibits the highest strength engages in direct interaction with the remaining three signals, so serving as the primary signal for decoding y_1 U1. The presentation provides information on the range of maximum values that can be achieved [30-31-32].

$$R_1 = \log_2\left(1 + \frac{\alpha_1 P|h_1|^2}{\alpha_2 P|h_1|^2 + \alpha_3 P|h_1|^2 + \alpha_4 P|h_1|^2 + +\alpha_5 P|h_1|^2 + \alpha_6 P|h_1|^2 + \sigma^2}\right) \quad (1)$$

where R is the NOMA rate download, α is the NOMA power location confection P is the transmit power, h is Rayleigh fading coefficients A is the antenna array gain.

In its most fundamental essence, this may be succinctly summarised.

$$R_1 = \log_2\left(1 + \frac{\alpha_1 P|h_1|^2}{(\alpha_2 + \alpha_3 + \alpha_4 + \alpha_5 + \alpha_6)P|h_1|^2 + \sigma^2}\right) \quad (2)$$

U2 refers to the rate that was reached after SIC had deleted U1 information.

$$R_2 = \log_2\left(1 + \frac{\alpha_2 P|h_2|^2}{(\alpha_3 + \alpha_4 + \alpha_5 + \alpha_6)P|h_2|^2 + \sigma^2}\right) \quad (3)$$

Subsequently, the inclusion of the α_3 term in the sentence should be removed. The subsequent rate provided pertains to U3:

$$R_3 = \log_2\left(1 + \frac{\alpha_3 P|h_3|^2}{(\alpha_4 + \alpha_5 + \alpha_6)P|h_3|^2 + \sigma^2}\right) \quad (4)$$

Following that, the α_4 inked to the aforementioned sentence must be eliminated. The subsequent figure represents the achievable rate for U4.

$$R_4 = \log_2\left(1 + \frac{\alpha_4 P|h_4|^2}{(\alpha_5 + \alpha_6)P|h_4|^2 + \sigma^2}\right) \quad (5)$$

Then, it is necessary to remove the term α_5 from the equation. The subsequent illustration showcases the attainable rate for the U5 category.

$$R_5 = \log_2\left(1 + \frac{\alpha_5 P|h_5|^2}{\alpha_6 P|h_5|^2 + \sigma^2}\right) \quad (6)$$

This is the U6 rate that can be considered acceptable:

$$R_6 = \log_2\left(1 + \frac{\alpha_6 P|h_6|^2}{\sigma^2}\right) \quad (7)$$

Obtain the SE using the formula given in [30].

$$SE = \frac{Th}{BW} \quad (8)$$

where SE stands for spectrum efficiency, Th is for throughput, and BW stands for bandwidth.

3.1. Uncooperative Cognitive Radio Network (Un-CCRN)

Spectrum sensing can come in a variety of forms, one of which is known as non-cooperative spectrum sensing. Other types of spectrum sensing include: (Energy Detector Sensing). Spectrum sensing carried out in this manner does not involve any collaboration between the many users or
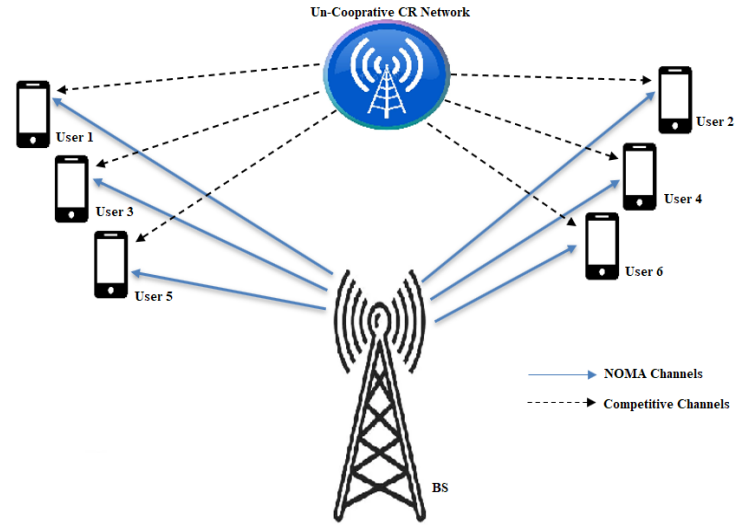
Figure 2. DL NOMA PD integrates the non-cooperative spectrum sensing network with six users

modules. Integration was carried out with the existing PD DL NOMA network, which counted a total of six users and was depicted in Figure 2 of the document.

A comparison is made between the output of the energy detector and a threshold that is determined by the noise level [16]. This comparison is carried out to determine whether or not the noise level has exceeded the threshold. The comparison enables the signal to be recognized and located. It begins by taking in a signal that goes by the name s(t) at the input, and then it proceeds to make a decision in the binary form regarding whether or not the PU is present. It is conceivable to represent it using [33] as a model.

$$z(t) = \begin{cases} n(t) & : H_0 \\ hs(t) + n(t), & : H_1 \end{cases} \quad (9)$$

where the transmitted signal, s(t), the additive noise signal, n(t), and the fading co-efficient of the channel, h, are all unknowns. H_1 indicates that the signal is present, whereas H_0 indicates that it is not.

The decision variable Z in ED is calculated by filtering, squaring, and integrating the signal z(t), which can also be expressed as:

$$z = c \int |z(t)|^2 \, dt \quad (10)$$

In the case of hypotheses H_0 and H_1, Specifically, Z's probability density function can be written as:

$$f_z(z) = \begin{cases} \dfrac{1}{2^u\,\Gamma(u)} z^{u-1} e^{-\frac{z}{2}} & :H_0 \\[2ex] \dfrac{1}{2}\left(\dfrac{z}{2Y}\right)^{\frac{u-1}{2}} e^{-\frac{2Y+z}{2}} I_{u-1}\left(\sqrt{2\gamma z}\right) & :H_1 \end{cases} \quad (11)$$

where I_r is the rth order Bessel function and $(\Gamma(u))$ is the gamma function. The secondary transmission SNR is denoted by Y.

We can calculate the detection probability and false alarm rate for AWGN fading channels using [32].

$$P_f = \frac{\Gamma\left(u,\frac{\lambda}{2}\right)}{\Gamma(u)} \quad (12)$$

$$P_d = Q_u\left(\sqrt{2\gamma},\sqrt{\lambda}\right) \quad (13)$$

where the wavelength (λ) is the detector threshold.

The generalized Marcum Q Function Q_u. The chance of detection for a Rayleigh distribution is expressed as [33].

$$P_{d}^{ray} = \frac{1}{1+\gamma} \Sigma_{n=1}^{u-1}\left(\frac{\lambda}{2}\right)^2 \frac{\exp\left(-\lambda/2\right)}{n!} |F|\left[1,n+1;\frac{\gamma\lambda}{2(1+\gamma)}\right] + \exp\left[-\frac{\lambda}{2(1+\lambda\gamma)}\right] \quad (14)$$

where $|F|$ is a hypergeometric function that is confluent, the secondary transmission SNR is denoted by γ, the wavelength (λ) is the detector threshold.

3.2 Cooperative Cognitive Radio Network (CCRN)

The primary goal of the CCRN is to improve detection efficiency, and the secondary goal is to make use of the natural variability that is present in observations made by geographically dispersed nodes of the CRN by employing the type of energy detector sensing methodology known as Cooperative Spectrum Sensing (CSS). Both of these goals are to be accomplished by utilising the CSS method.

The primary objective of the CCRN is to capitalise on the natural degree of uncertainty that is present in CRN node measurements. The nodes that make up a CRN pool their sensor data and share it; as a result, it is possible to make judgements that are more informed than those that could be reached using information from a single source on its own. Figure 3 of this paper presents a representation of the author's combination with an earlier PD-DL NOMA network that included a total of six users.
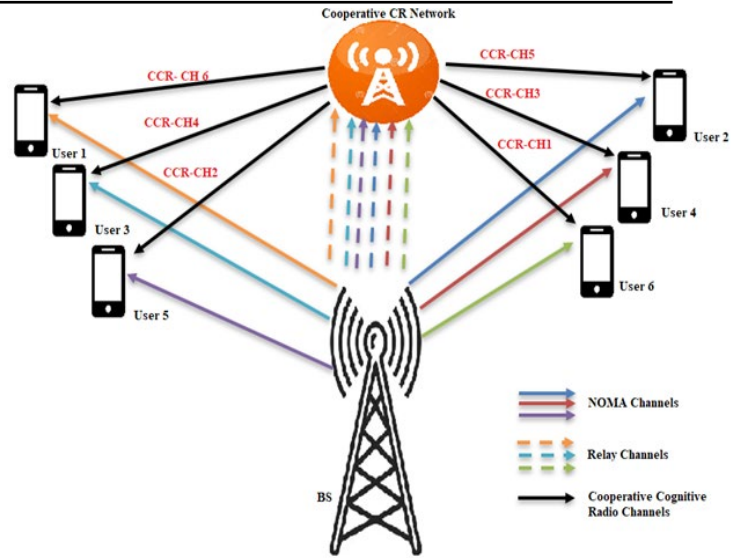

Figure 3. CSS network with six users is integrated into DL NOMA PD

Let $D_i \in \{0, 1\}$'s denote the local spectrum sensing result of the i_{th} CR. All 1-bit decisions are fused according to the following logical rule [31]:

$$Y = \Sigma_{i=1}^{k} D_i \quad (15)$$

where Y is the decision variable and D_i is the decision of CR.

The overall detection and false alarm probability when employing the k-out-of-N fusion rule is provided in the reference [33-34]. The reason why this is the case is because the rule takes into account every potential combination of the inputs, which is the reason why this is the case.

$$Q_f = \Sigma_{i=k}^{N} \binom{N}{i} P_f^{i} \left(1-P_f\right)^{N-i} \quad (16)$$

$$Q_d = \Sigma_{i=k}^{N} \binom{N}{i} P_d^{i} \left(1-P_d\right)^{N-i} \quad (17)$$

The chance of detecting a signal is commonly represented by the variable Q_d, while the likelihood of a false alarm is typically symbolised by the symbol Q_f. The base station is capable of inferring the presence of a primary user signal whenever there is at least one cognitive radio that aligns with the local decision H1.

3.3 M-MIMO NOMA System

In this part, it is assumed that the wireless network contains 6 users U1, U2, U3, U4, U5, and U6 and $(\alpha_2 < \alpha_1, \alpha_3 < \alpha_2, \ldots, \alpha_6 < \alpha_5)$ is spread out at various distances, each using a 128x128, 256x256, and 512x512 M-MIMO DL NOMA PD, and all of these users are contained within one cell. Other networks from uncooperative and cooperative CR-NOMA have been added to complete the integration.
The transmit signal is

$$x = \sqrt{P}\left(\sqrt{\alpha_1}x_1 + \sqrt{\alpha_2}x_2 + \sqrt{\alpha_3}x_3 + \sqrt{\alpha_4}x_4 + \sqrt{\alpha_5}x_5 + \sqrt{\alpha_6}x_6\right) \quad (18)$$

The relevant variables are denoted as x1, x2, x3, x5, and x6. Each entity's power coefficients are denoted as α1, α2, α3, α4, α5, and α6.

The signal was obtained by the BS.

$$y = \sqrt{P_{x1}}h_{16} + \sqrt{P_{x2}}h_{26} + \sqrt{P_{x3}}h_{36} + \sqrt{P_{x4}}h_{46} + \sqrt{P_{x5}}h_{56} + \sqrt{P_{x6}}h_{66} \quad (19)$$

4. Simulation Parameters

In Table 1, you will find a listing of all of the simulation parameters that were used for each of the three distinct networks, as well as the values that correspond to those parameters.

Table 1. Table 1 contains a listing of all of the simulation parameters that were utilised for each of the three different networks

Parameters	Values
Users Number	6
Distances between users and BS	(1750, 1500, 1250, 1000, 750, 500) m
Power Transmit (BS)	0 to 30 dBm
Path loss exponent	4
Modulation	QPSK
Bandwidth	70MHz
Massive-MIMO	128x128, 256x256, 512x512
Power location coefficients for users	0,7, 0.225, 0.056, 0.014, 0.0035, 0.00087

5. Results and Discussion

The following figures show how the SE evaluation relates to transmitting power for DL NOMA PD, DL uncooperative CR-NOMA, and DL cooperative CR-NOMA using 128x128, 256x256, and 512x512 M-MIMO, respectively. These findings are predicated on running the software in each of the three network configurations.

5.1 DL NOMA PD Model Results

Figure 4 displays the SE versus transmit power (TP)for four users (U1, U2, U3, U4, U5, and U6) in DL NOMA PD with an unstable channel state at distances of 1750 m, 1500 m, 1250 m, 1000 m, 750 m, and 500 m with power location coefficients of (0.7), (0.225), (0.056), (0.014), (0.00035), and (0.00087) According to the findings, the SE rose in proportion to the increasing TP. U6, the radio that is nearest to the BS, provides the highest SE results at 40 dBm, with 5.51 bps/Hz. After this comes U5, then U4, U3, U2, and finally U1.

Figure 5 illustrates the effect of the DL NOMA PD in combination with the uncooperative CRN by displaying the SE as a result of transmitting power for six users. U6's best SE performance is 6.07 bps/Hz when transmitted with 30 dBm of power.

Figure 6 depicts the SE against TP for DL NOMA PD combined with the cooperative CRN for six users. With a TP of 30 dBm, the highest SE result is 6.67 bps/Hz for U6. The observed results outperform the results found in the references [35] on the performance of the SE.
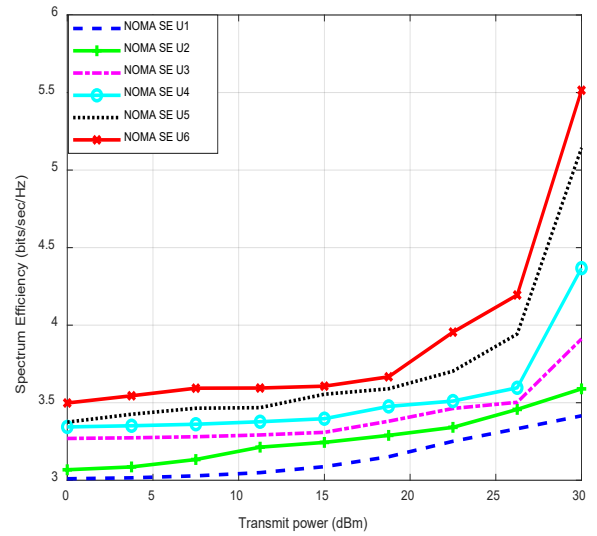

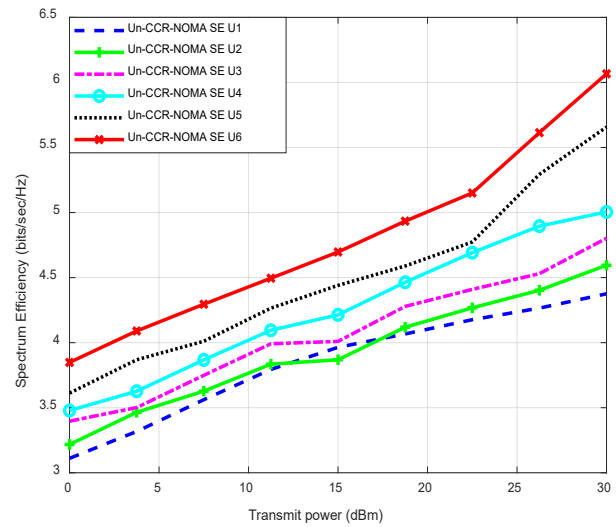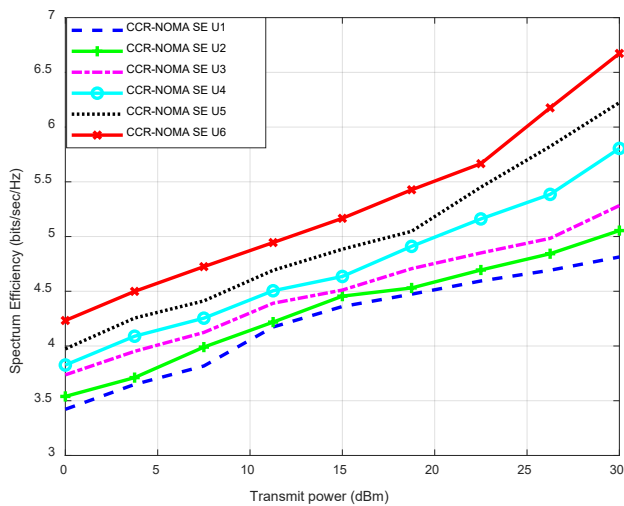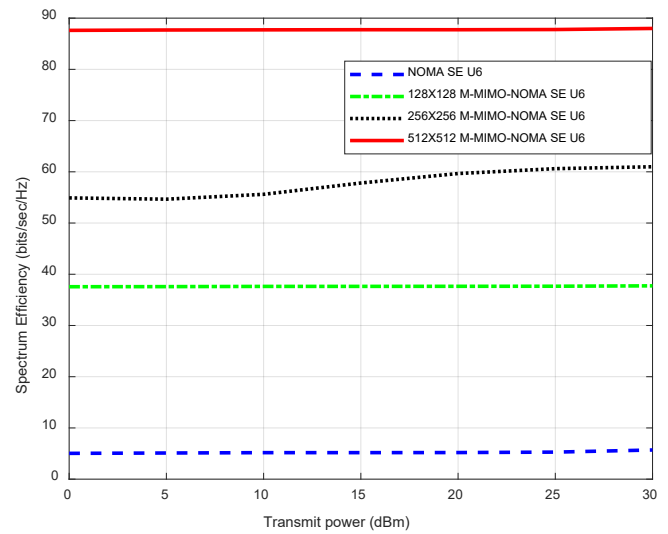**Figure 4.** SE against TR in the DL NOMA network with 6 users

Figure 5. SE versus TR for 6 DL NOMA users on the UC-CRN

Figure 6. SE vs. TR for 6 users DL NOMA PD with CCRN

**Figure 7.** SE against TR for U6 DL NOMA PD network with 128x128, 256x256 and 512x512 M-MIMO schemes

5.2 M-MIMO DL NOMA PD Model Results

Figure 7 presents a comparison between the SE and the TP result obtained from the best user (U6) in DL NOMA PD, 128x128, 256x256, and 512x512 M-MIMO with an unstable channel state at constant distances and power location coefficients. When the TP goes up, the SE also goes up. After implementing the 128x128, 256x256, and 512x512 MIMO technologies with DL NOMA, the SE of the U6 increased by 73%, 82%, and 87%, respectively, as compared to the U6's performance using DL NOMA PD. These improvements were achieved at a transmitting power of 30 dBm.

Figure 8 presents a comparison between the SE and the TP result obtained by the best user (U6) in DL uncooperative CR-NOMA PD with, 128x128, 256x256, and 512x512 M-MIMO. When compared to the performance of the SE for U6 when it was using DL uncooperative CR-NOMA PD, the SE increased by 75%, 83%, and 88%, respectively, after implementing the 128x128, 256x256, and 512x512 M-MIMO technologies with DL uncooperative CR-NOMA. These enhancements were accomplished while the transmitting power was set at 30 dBm.

Figure 9 presents the outcome of comparing the SE to the TP. As the transmitting power is raised, the SE also rises. With the implementation of 128x128, 256x256, and 512x512 M-MIMO technologies utilizing DL cooperative CR-NOMA PD, the SE for U6 rose by 75.8%, 84%, and 88.3%, respectively, at the TP of 30 dBm, compared to its performance while using DL cooperative CR-NOMA PD.

The outcomes that were gathered had a greater level of significance than the SE performance that was utilized as a reference [36-37-38].
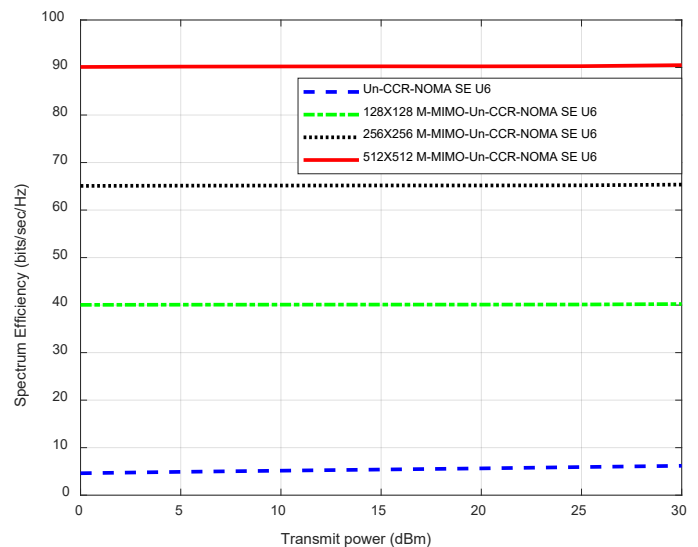
Figure 8. SE versus TR for U6 DL un-cooperative CR- NOMA PD network with 128x128, 256x256 and 512x512 M-MIMO schemes
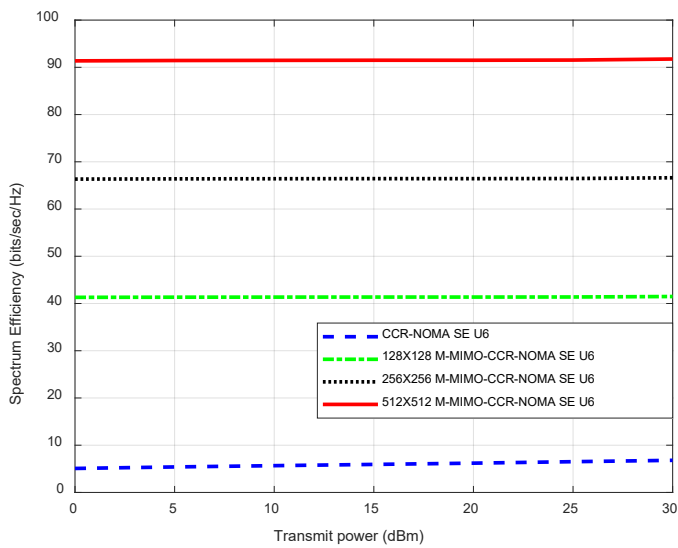
Figure 9. SE vs. TR for U6 DL cooperative CR- NOMA PD network with 128x128, 256x256 and 512x512 M-MIMO schemes

6. Conclusions and Future Work

This paper explores the SE of DL NOMA PD in the 6G network equipped with 128x128, 256x256, and 512x512 M-MIMO technologies paired with the uncooperative and cooperative CRN by utilizing a novel methodology. Every user has a unique combination of TP, distance, and power location coefficients. In especially, the SIC and unstable channels, as well as Rayleigh fading and AWGN, were taken into consideration during the performance evaluation. According to the findings of the DL NOMA system, the performance of SE was significantly improved by the integration of M-MIMO with NOMA, as well as by both uncooperative and cooperative CR-NOMA. At 30 dBm of TP, the results show that the user U6 achieves the best SE performance of 5.51 bits/sec/Hz in DL NOMA, 6.07 bits/sec/Hz in DL uncooperative CR-NOMA, and 6.67 bits/sec/Hz in DL cooperative CR-NOMA NOMA. At 30 dBm TP, the SE performance for U6 best use was enhanced by 37.7 bits/sec/Hz due to DL 128x128 M-MIMO NOMA, but DL 128x128 M-MIMO uncooperative CR-NOMA enhanced SE performance by 40.2 bits/sec/Hz and DL 128x128 M-MIMO cooperative CR-NOMA improved SE performance by 41.5 bits/sec/Hz. With the best use of U6, the performance of DL 256x256 M-MIMO NOMA increased by 60.98 bits/sec/Hz when relative to the SE performance of DL NOMA; DL 256x256 M-MIMO uncooperative CR-NOMA enhanced it by 65.4 bits/sec/Hz; and DL 256x256 M-MIMO cooperative CR-NOMA improved it by 66.61 bits/sec/Hz, at 30 dBm TP. Whereas DL 512x512 M-MIMO NOMA enhanced SE performance for U6 the best use by 41.5 bits/sec/Hz, DL 512x512 M-MIMO un-cooperative CR-NOMA improved the SE

performance by 66.61 bits/sec/Hz, while DL 512x512 M-MIMO cooperative CR-NOMA enhanced the SE performance by 91.8 bits/sec/Hz, at 30 dBm TP as the comparison to DL NOMA's SE performance. Results from the DL NOMA system confirmed that combining with proposer strategies significantly enhanced SE performance.

In comparison to the U6's performance with DL NOMA PD at the TP of 30 dBm, the SE of the U6 increased by 73%, 82%, and 87%, respectively, after integrating the 128x128, 256x256, and 512x512 MIMO technologies with DL NOMA. The highest user (U6) in DL non-cooperative CR-NOMA PD has 128x128, 256x256, and 512x512 M-MIMO. After implementing the 128x128, 256x256, and 512x512 M-MIMO technologies with DL uncooperative CR-NOMA at TP of 30 dBm, the SE for U6 improved by 75%, 83%, and 88%, respectively, in comparison to the performance of the SE when it was utilizing DL uncooperative CR-NOMA PD. The SE for U6 increased by 75.8%, 84%, and 88.3%, respectively, at the TP of 30 dBm after implementing 128x128, 256x256, and 512x512 M-MIMO technologies using DL cooperative CR-NOMA PD, compared to its performance when using DL cooperative CR-NOMA PD.

Future research will focus on adding both uncooperative and cooperative DL-CR-cooperative NOMA to massive MIMO.

References

[1] S. Mumtaz et al., "Terahertz communication for vehicular networks", *IEEE Trans. Veh. Technol.*, vol. 66, pp. 5617-5625, Jul. 2017.
[2] W. Saad, M. Bennis and M. Chen, "A vision of 6G wireless systems: Applications trends technologies and open research problems", *IEEE Netw.*, vol. 34, no. 3, pp. 134-142, May/Jun. 2020.
[3] G. Gui, H. Sari and E. Biglieri, "A New Definition of Fairness for Non-Orthogonal Multiple Access," in IEEE Communications Letters, vol. 23, no. 7, pp. 1267-1271, July 2019, doi: 10.1109/LCOMM.2019.2916398.
[4] M. Hassan, M. Singh and K. Hamid, "Survey on NOMA and Spectrum Sharing Techniques in 5G," 2021 IEEE International Conference on Smart Information Systems and Technologies (SIST), Nur-Sultan, Kazakhstan, 2021, pp. 1-4, doi: 10.1109/SIST50301.2021.9465962.
[5] G. Gui, H. Sari and E. Biglieri, "A New Definition of Fairness for Non-Orthogonal Multiple Access," in IEEE Communications Letters, vol. 23, no. 7, pp. 1267-1271, July 2019, doi:10.1109/LCOMM.2019.2916398.
[6] Q. Wang, R. Zhang, L. -L. Yang and L. Hanzo, "Non-Orthogonal Multiple Access: A Unified Perspective," in IEEE Wireless Communications, vol. 25, no. 2, pp. 10-16, April 2018, doi: 10.1109/MWC.2018.1700070.
[7] P. N. Thakre and S. B. Pokle, "A survey on Power Allocation in PD-NOMA for 5G Wireless

Communication Systems," 2022 10th International Conference on Emerging Trends in Engineering and Technology - Signal and Information Processing (ICETET-SIP-22), Nagpur, India, 2022, pp. 1-5, doi: 10.1109/ICETET-SIP-2254415.2022.9791576.

[8] L. Dai, B. Wang, Z. Ding, Z. Wang, S. Chen and L. Hanzo, "A Survey of Non-Orthogonal Multiple Access for 5G," in IEEE Communications Surveys & Tutorials, vol. 20, no. 3, pp. 2294-2323, thirdquarter 2018, doi: 10.1109/COMST.2018.2835558.

[9] K. Chung, "Correlated Superposition Coding: Lossless Two-User NOMA Implementation Without SIC Under User-Fairness," in IEEE Wireless Communications Letters, vol. 10, no. 9, pp. 1999-2003, Sept. 2021, doi: 10.1109/LWC.2021.3089996.

[10] H. Haci, H. Zhu and J. Wang, "Performance of Non-orthogonal Multiple Access With a Novel Asynchronous Interference Cancellation Technique," in IEEE Transactions on Communications, vol. 65, no. 3, pp. 1319-1335, March 2017, doi: 10.1109/TCOMM.2016.2640307.

[11] X. Chen, R. Jia and D. W. K. Ng, "On the Design of Massive Non-Orthogonal Multiple Access With Imperfect Successive Interference Cancellation," in IEEE Transactions on Communications, vol. 67, no. 3, pp. 2539-2551, March 2019, doi: 10.1109/TCOMM.2018.2884476.

[12] S. Rezvani, E. A. Jorswieck, R. Joda and H. Yanikomeroglu, "Optimal Power Allocation in Downlink Multicarrier NOMA Systems: Theory and Fast Algorithms," in IEEE Journal on Selected Areas in Communications, vol. 40, no. 4, pp. 1162-1189, April 2022, doi: 10.1109/JSAC.2022.3143237.

[13] D. H. Tashman and W. Hamouda, "An Overview and Future Directions on Physical-Layer Security for Cognitive Radio Networks," in IEEE Network, vol. 35, no. 3, pp. 205-211, May/June 2021, doi: 10.1109/MNET.011.2000507.

[14] M. Hassan, M. Singh, K. Hamid, "Overview of Cognitive Radio Networks, " Journal of Physics: Conference Series, International Conference on Robotics and Artificial Intelligence (RoAI) 28-29 December, Chennai, India, vol. 1831, 2020, doi: 10.1088/1742-6596/1831/1/012013.

[15] M. Hassan, M. Singh, K. Hamid, "Survey on Advanced Spectrum Sharing Using Cognitive Radio Technique, " In: Tuba, M., Akashe, S., Joshi, A. (eds) ICT Systems and Sustainability. Advances in Intelligent Systems and Computing, vol 1270. Springer, Singapore. doi:10.1007/978-981-15-8289-9_62.

[16] W. Liang, S. X. Ng and L. Hanzo, "Cooperative Overlay Spectrum Access in Cognitive Radio Networks," in IEEE Communications Surveys & Tutorials, vol. 19, no. 3, pp. 1924-1944, thirdquarter 2017, doi: 10.1109/COMST.2017.2690866.

[17] W. S. H. M. W. Ahmad et al., "5G Technology: Towards Dynamic Spectrum Sharing Using Cognitive Radio Networks," in IEEE Access, vol. 8, pp. 14460-14488, 2020, doi: 10.1109/ACCESS.2020.2966271.

[18] L. Lv, Q. Ni, Z. Ding and J. Chen, "Application of Non-Orthogonal Multiple Access in Cooperative Spectrum-Sharing Networks Over Nakagami-m Fading Channels," in IEEE Transactions on Vehicular Technology, vol. 66, no. 6, pp. 5506-5511, June 2017, doi: 10.1109/TVT.2016.2627559.

[19] L. Lv, J. Chen, Q. Ni and Z. Ding, "Design of Cooperative Non-Orthogonal Multicast Cognitive Multiple Access for 5G Systems: User Scheduling and Performance Analysis," in IEEE Transactions on Communications, vol. 65, no. 6, pp. 2641-2656, June 2017, doi: 10.1109/TCOMM.2017.2677942.

[20] Y. Tang, Y. Huang, M. Wen, L. -L. Yang and C. -B. Chae, "A Molecular Spatio-Temporal Modulation Scheme for MIMO Communications," 2021 IEEE Wireless Communications and Networking Conference (WCNC), 2021, pp. 1-6, doi: 10.1109/WCNC49053.2021.9417557.

[21] G. Kaddoum, Y. Nijsure and H. Tran, "Generalized Code Index Modulation Technique for High-Data-Rate Communication Systems," in IEEE Transactions on Vehicular Technology, vol. 65, no. 9, pp. 7000-7009, Sept. 2016, doi: 10.1109/TVT.2015.2498040.

[22] A. J. Moshayedi, Z. -Y. Chen, L. Liao and S. Li, " Sunfa Ata Zuyan machine learning models for moon phase detection: algorithm, prototype and performance comparison, " TELKOMNIKA Telecommunication Computing Electronics and Control, Vol. 20, No. 1, February 2022, pp. 129~140, ISSN: 1693-6930, doi: 10.12928/TELKOMNIKA.v20i1.22338.

[23] A. J. Moshayedi, Z. -Y. Chen, L. Liao and S. Li, "Portable Image Based Moon Date Detection and Declaration: System and Algorithm Code Sign," *2019 IEEE International Conference on Computational Intelligence and Virtual Environments for Measurement Systems and Applications (CIVEMSA)*, Tianjin, China, 2019, pp. 1-6, doi: 10.1109/CIVEMSA45640.2019.9071604.

[24] A. J. Moshayedi, A. S. Khan, S. Yang and S. M. Zanjani, "Personal Image Classifier Based Handy Pipe Defect Recognizer (HPD): Design and Test," 2022 7th International Conference on Intelligent Computing and Signal Processing (ICSP), Xi'an, China, 2022, pp. 1721-1728, doi: 10.1109/ICSP54964.2022.9778676.

[25] Y. Liu, Q. Zhang, X. He, al. et, " Spectral-efficient hybrid precoding for multi-antenna multi-user mmWave massive MIMO systems with low complexity," J Wireless Com Network 2022, 66 (2022). doi:10.1186/s13638-022-02150-2.

[26] F. Zhang, M. M. Wang, X. Bao and W. Liu, "Centralized Resource Allocation and Distributed Power Control for NOMA-Integrated NR V2X," in IEEE Internet of Things Journal, vol. 8, no. 22, pp. 16522-16534, 15 Nov.15, 2021, doi: 10.1109/JIOT.2021.3075250.

[27] Z. Zhou, H. Yu, S. Mumtaz, S. Al-Rubaye, A. Tsourdos and R. Q. Hu, "Power Control Optimization for Large-Scale Multi-Antenna Systems," in IEEE Transactions

on Wireless Communications, vol. 19, no. 11, pp. 7339-7352, Nov. 2020, doi: 10.1109/TWC.2020.3010701.

[28] Sousa de Sena, D. B. da Costa, Z. Ding, P. H. J. Nardelli, U. S. Dias and C. B. Papadias, "Massive MIMO-NOMA Networks With Successive Sub-Array Activation," in IEEE Transactions on Wireless Communications, vol. 19, no. 3, pp. 1622-1635, March 2020, doi: 10.1109/TWC.2019.2955647.

[29] L. Zhou, J. Dai, W. Xu and C. Chang, "Sparse Channel Estimation for Intelligent Reflecting Surface Assisted Massive MIMO Systems," in IEEE Transactions on Green Communications and Networking, vol. 6, no. 1, pp. 208-220, March 2022, doi: 10.1109/TGCN.2022.3146188.

[30] M. Hassan, M. Singh, and Kh. Hamid , "BER Performance of NOMA Downlink for AWGN and Rayleigh Fading Channels in (SIC)," in MCA, EAI, 2022, doi: 10.4108/eai.20-6-2022.174227.

[31] M. Hassan, M. Singh, Kh. Hamid, R. Saeed, M. Abdelhaq, and R.Alsaqour," Design of Power Location Coefficient System for 6G Downlink Cooperative NOMA Network," Energies, 2022, 15(19), 6996; doi:10.3390/en15196996.

[32] M. Hassan, M. Singh, Kh. Hamid, R. Saeed, M. Abdelhaq, and R.Alsaqour," Modeling of NOMA-MIMO-Based Power Domain for 5G Network under Selective Rayleigh Fading Channels," Energies 2022, 15, 5668, doi:10.3390/en15155668.

[33] K. Cheng, L. Zhu, W. Wang and P. Chen, "CCSAE-Based Un-Cooperative Communication Behavior Recognition Scheme," 2022 7th International Conference on Computer and Communication Systems (ICCCS), Wuhan, China, 2022, pp. 741-745, doi: 10.1109/ICCCS55155.2022.9846728.

[34] X. Liu, M. Jia, Z. Na, W. Lu and F. Li, "Multi-Modal Cooperative Spectrum Sensing Based on Dempster-Shafer Fusion in 5G-Based Cognitive Radio," in IEEE Access, vol. 6, pp. 199-208, 2018, doi: 10.1109/ACCESS.2017.2761910.

[35] Sousa de Sena, D. Benevides da Costa, Z. Ding and P. H. J. Nardelli, "Massive MIMO–NOMA Networks With Multi-Polarized Antennas," in IEEE Transactions on Wireless Communications, vol. 18, no. 12, pp. 5630-5642, Dec. 2019, doi: 10.1109/TWC.2019.2937868.

[36] Shen, D.; Wei, C.; Zhou, X.; Wang, L.; Xu, C. Photon Counting Based Iterative Quantum Non-Orthogonal Multiple Access with Spatial Coupling. In Proceedings of the 2018 IEEE Global Communications Conference (GLOBECOM), Abu Dhabi, United Arab Emirates, 9–13 December 2018; pp. 1–6.

[37] Dinh, S., Liu, H., Ouyang, F. (2019). Massive mimo cognitive cooperative relaying. In: Biagioni, E., Zheng, Y., Cheng, S. (eds) Wireless Algorithms, Systems, and Applications. WASA. Lecture Notes in Computer Science, vol 11604. Springer.

[38] Mona, B., Elmustafa S., Rashid A. S. (2020). Ultra-Massive mimo in thz communications, Book: Next generation wireless terahertz communication networks, CRC group, Taylor & Francis Group, USA.